Element and orbital-specific observation of two-step magnetic transition in $NpNiGa_5$: X-ray magnetic circular dichroism study

T. Okane,[1,*] T. Ohkochi,[1,†] T. Inami,[1] Y. Takeda,[1] S.-i. Fujimori,[1] N. Kawamura,[2] M. Suzuki,[2] S. Tsutsui,[2] H. Yamagami,[1,3] A. Fujimori,[1,4] A. Tanaka,[5] D. Aoki,[6,‡] Y. Homma,[6] Y. Shiokawa,[6] E. Yamamoto,[7] Y. Haga,[7] A. Nakamura,[7] and Y. Ōnuki[7,8]

[1]*Synchrotron Radiation Research Center, Japan Atomic Energy Agency, Hyogo 679-5148, Japan*
[2]*SPring-8/Japan Synchrotron Radiation Research Institute, Hyogo 679-5198, Japan*
[3]*Department of Physics, Kyoto Sangyo University, Kyoto 603-8555, Japan*
[4]*Department of Physics, University of Tokyo, Tokyo 113-0033, Japan*
[5]*Department of Quantum Matters, ADSM, Hiroshima University, Hiroshima 739-8530, Japan*
[6]*Institute for Materials Research, Tohoku University, Ibaraki 311-1313, Japan*
[7]*Advanced Science Research Center, Japan Atomic Energy Agency, Ibaraki 319-1195, Japan*
[8]*Department of Physics, Osaka University, Toyonaka, Osaka 560-0043, Japan*

(Received 4 June 2009; revised manuscript received 10 August 2009; published 16 September 2009)

X-ray magnetic circular dichroism (XMCD) experiments were performed at the Np $M_{4,5}$ and the Ga K absorption edges of $NpNiGa_5$ to investigate the temperature-dependent changes of magnetic properties of Np $5f$ and Ga $4p$ electron states. By the sum-rule analysis of the Np $M_{4,5}$ XMCD data, the orbital magnetic moment μ_L and the spin magnetic moment μ_S were estimated for the Np $5f^3$ and $5f^4$ electronic configurations and their comparison to the previous magnetization and neutron-scattering experiments suggests that the $5f^4$ configuration is more likely than the $5f^3$ configuration in $NpNiGa_5$. It was found that $|\mu_L/\mu_S|$ tends to increase from the high-temperature low-moment ordered state to the low-temperature high-moment ordered state. The result of the Ga K XMCD indicates that the Ga $4p$ electrons are magnetically polarized and the temperature and magnetic-field dependences of the Ga $4p$ orbital moment are proportional to those of the magnetization measurements.

DOI: 10.1103/PhysRevB.80.104419 PACS number(s): 71.27.+a, 75.20.Hr, 75.30.Kz, 78.70.Dm

I. INTRODUCTION

Actinide-based 115-type compounds $AnTGa_5$ (An =actinides; T=transition metals), crystallizing in the tetragonal $HoCoGa_5$ structure, have been actively investigated since the discovery of superconductivity in $PuCoGa_5$ and $PuRhGa_5$ with relatively high critical transition temperatures of T_c=18.5 K and 8 K, respectively.[1,2] $NpTGa_5$ compounds show complicated magnetic orderings such as metamagnetism and multiple magnetic phase transitions,[3–10] while $UTGa_5$ compounds exhibit Pauli paramagnetism or antiferromagnetism.[11–16] Because superconductivity has not been found in $UTGa_5$ and $NpTGa_5$, it is an interesting issue why only Pu 115 compounds exhibit superconductivity. The superconductivity would be closely related to the delocalized nature of $5f$ electrons. Magnetometry and electrical transport experiments for An-substituted and T-substituted $PuCoGa_5$ suggested that the variation of critical temperature or critical field in superconductivity is related to the total electron number.[17] Because $NpNiGa_5$ has the same total electron number as in $PuCoGa_5$, the mechanism of the magnetic behavior of $NpNiGa_5$ would be an important clue to understand the relationship between magnetism and superconductivity in $PuCoGa_5$.

$NpNiGa_5$ is a heavy Fermion compound as implied by the large electronic specific coefficient $\gamma \sim 100$ mJ/mol K^2,[6,7] that is the highest among the $NpTGa_5$ compounds and comparable to those of $PuCoGa_5$ and $PuRhGa_5$.[18,19] $NpNiGa_5$ exhibits successive magnetic ordering. As the temperature is lowered, the magnetization along the easy axis, namely, the c axis, markedly increases at the two temperatures, 30 and 18 K.[6,7] Previous neutron-scattering experiments suggested that the low-moment (LM) state in the temperature range 18 K $<T<$ 30 K (T_C) is attributed to the ferromagnetic (FM) state, where the magnetic moments are aligned along the c axis, as shown in Fig. 1(a), and that the high-moment (HM) state in the temperature range $T<$ 18 K (T_N) is in the canted antiferromagnetic (AFM) state, where the magnetic moments are tilted toward the a axis and the in-plane components have an AFM order, as shown in Fig. 1(b).[10] An interesting point is that, in the canted AFM phase, the projected moment along the c axis is larger than that in the FM phase, even though the moment direction is canted away from the c axis. It is expected that the Np $5f$ electronic states change at the

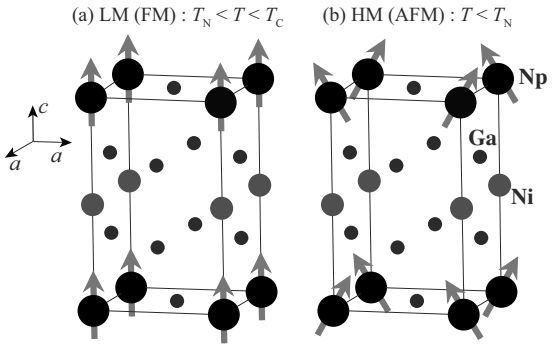

FIG. 1. Magnetic structures of $NpNiGa_5$ proposed in Ref. 10. (a) LM–FM phase at $T_N<T<T_C$. (b) HM–canted AFM phase at $T<T_N$.

FM→AFM phase transition, presumably accompanied by a Fermi-surface reconstruction.[10]

In order to understand what drives the FM→AFM ordering of $NpNiGa_5$, it is essential to clarify details of the Np $5f$ electron states in the two different magnetically ordered states and the difference between them, since the magnetic properties of those *An*-based compounds are dominated by the nature of *An* $5f$ electrons. X-ray magnetic circular dichroism (XMCD) is a useful tool to investigate the magnetic properties of a certain electron orbital of a specific element in a compound. Therefore, we have performed the XMCD study at the Np $M_{4,5}$ ($3d \rightarrow 5f$) absorption edges, which provides information about the Np $5f$ electrons. Analysis of the $M_{4,5}$ XMCD data utilizing the orbital and spin sum rules[20,21] enables us to estimate the orbital magnetic moment μ_L and the spin magnetic moment μ_S of the $5f$ electrons separately. Since the sizable orbital magnetic moment induced by the strong spin-orbit interaction is one of the characteristics of actinide compounds, separate estimations of μ_L and μ_S are the key to interpreting their magnetic properties, which depends on the degree of delocalization of the $5f$ electrons. In addition, XMCD at the Ga K edge ($1s \rightarrow 4p$) can be used to investigate the contribution of p electrons of the ligand element to the magnetic properties. The Ga $4p$ electrons would be magnetically polarized through hybridization with *An* $5f$ electron states.[22,23] The magnetic polarization of the Ga $4p$ electrons was previously reported from the resonant x-ray scattering study for $UTGa_5$ (T=Ni, Pd, and Pt) (Ref. 24) and $NpTGa_5$ (T=Rh and Co).[25] We have examined the possibility of using Ga K XMCD data as a probe of the $5f$ magnetic moment in actinide compounds.

II. EXPERIMENT

The measured sample was a single crystal grown by the procedure described in Ref. 6. The XMCD measurements at the Np $M_{4,5}$ and Ga K absorption edges were performed at beamlines BL22XU and BL39XU, respectively, of SPring-8. In the XMCD measurements, circularly polarized x rays, which were produced by a diamond x-ray phase retarder, irradiated the sample along the c axis and a magnetic field of 0.1 T, which was sufficient to saturate the magnetization along the c axis,[6] was applied along the c axis using a superconducting magnet. The x-ray absorption spectra (XAS) were obtained by the fluorescence-yield method using a silicon drift detector. The XMCD signals were obtained by reversing the helicity of x-ray photons under the fixed direction of the magnetic field or by reversing the direction of the magnetic field under the fixed x-ray helicity.

In the fluorescence-yield measurements, the intensity modulation of the XAS spectra due to self-absorption is significant and the intensity ratio of the M_5 ($3d_{5/2}$) signal to the M_4 ($3d_{3/2}$) signal may remarkably deviate from the intrinsic value.[26] In the present study, the data analysis was carried out under the assumption that the ratio of the integrated XAS intensity at the M_5 edge to that at the M_4 edge satisfies the branching ratio B=0.760 for n_f=4 or 0.723 for n_f=3, obtained from relativistic atomic Hartree-Fock calculations in intermediate coupling, calculated for the $N_{4,5}$ edges.[27] Here,

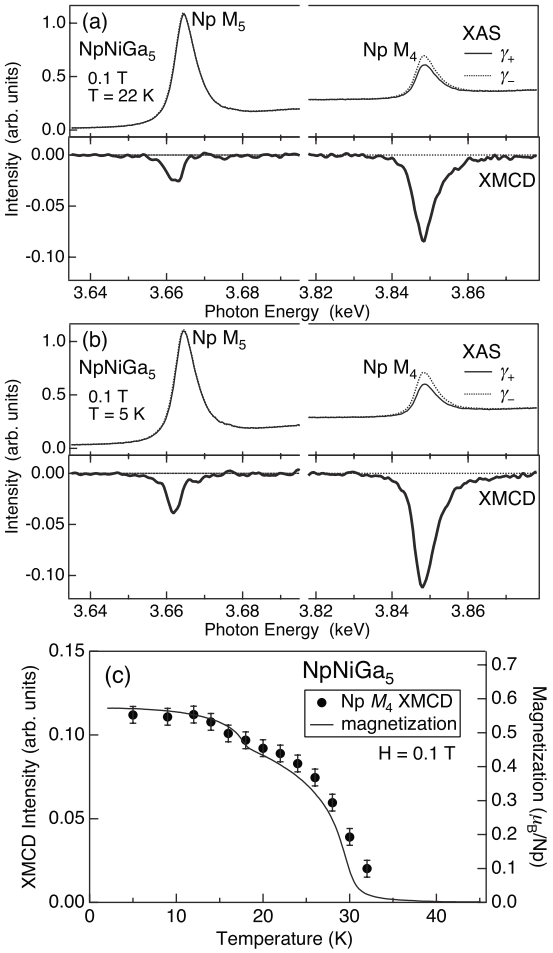

FIG. 2. XAS and XMCD spectra at the Np $M_{4,5}$ edges of $NpNiGa_5$ measured at (a) 22 K and (b) 5 K. γ_+ and γ_- denote XAS spectra measured with the photon helicity parallel and antiparallel to the magnetic field of 0.1 T applied along the c axis, respectively. The XMCD spectra are obtained as $\Delta\gamma = \gamma_+ - \gamma_-$. Each spectrum has been normalized to the unity at the M_5 peak of the XAS spectrum. (c) Temperature dependence of the intensity of the Np M_4 XMCD signal of $NpNiGa_5$ under a magnetic field applied along the c axis compared to the temperature dependence of the magnetization along the c axis (Ref. 6).

$B \equiv A_{5/2}/(A_{5/2}+A_{3/2})$, where $A_{5/2}$ and $A_{3/2}$ are the integrated intensities of the M_5 and the M_4 XAS signals, respectively, and n_f is the $5f$ electron occupation number.

III. RESULTS

A. Np $M_{4,5}$ XMCD

Figures 2(a) and 2(b) show the Np $M_{4,5}$ XAS and XMCD spectra of $NpNiGa_5$ measured at 22 K (LM state) and 5 K (HM state), respectively. The XAS spectra measured with the photon helicity parallel and antiparallel to the direction of the magnetization are denoted by γ_+ and γ_-, respectively. The XMCD spectra were obtained as the difference $\Delta\gamma = \gamma_+ - \gamma_-$. The XAS spectra have simple line shapes composed of two white-line peaks without appreciable fine structures due to multiplet splitting. The line shapes of the $M_{4,5}$ XMCD spec-

TABLE I. Values of the 5*f*-electron magnetic moments along the *c* axis in units of μ_B estimated using the sum-rule analysis of the XMCD data at the Np $M_{4,5}$ edges of $NpNiGa_5$ at 22 K (the LM state) and 5 K (the HM state). The μ_{TOT} values along the *c* axis obtained from the previous magnetization (Ref. 6) and neutron-scattering (Ref. 10) experiments and the μ_S values obtained from the magnetic Compton scattering experiment (Ref. 40) are also listed (Ref. 42).

	22 K (LM state)				5 K (HM state)			
	μ_L	μ_S	μ_{TOT}	μ_L/μ_S	μ_L	μ_S	μ_{TOT}	μ_L/μ_S
5 f^3 (Np^{4+})	0.97	−0.38	0.59	−2.57	1.35	−0.50	0.85	−2.70
$5f^4$ (Np^{3+})	0.79	−0.45	0.34	−1.76	1.10	−0.59	0.51	−1.88
Magnetization (Ref. 6)			0.40				0.57	
Neutron (Ref. 10)			0.32				0.47	
Compton (Ref. 40)		−0.44[a]				−0.41		

[a]Measured at 20 K.

tra of $NpNiGa_5$ show the following characteristics:

(1) The XMCD signals at the M_5 and M_4 edges have the same sign (negative in the figure).

(2) The XMCD signal at the M_4 edge has a much larger intensity than that at the M_5 edge.

(3) While the XMCD signal at the M_4 edge has line shapes similar to the line shapes of the M_4 XAS spectra (same peak position), the XMCD signal at the M_5 edge has asymmetric line shapes clearly different from the line shapes of M_5 XAS spectra.

These observations are similar to those observed in the $M_{4,5}$ and $N_{4,5}$ XMCD spectra of magnetic uranium compounds.[26,28–35] The first and second observations indicate an antiparallel coupling between μ_L and μ_S. From analogy with the result of the uranium compounds,[36,37] the third observation implies that the asymmetric line shapes of the M_5 signal might be sensitive to the environment of the 5*f* electrons. The intensity of the XMCD signal becomes larger in going from the LM state to the HM state, reflecting the increase of the magnetization along the *c* axis.

Figure 2(c) shows the temperature dependence of the intensity of the M_4 XMCD signal. As the temperature is lowered, the intensity rapidly rises around 30 K. After saturation around the temperature below 25 K, the intensity obviously increases again around 15 K. Thus, the two-step magnetic transition in the magnetization measurements was observed also in the intensity variation of the XMCD signal. This confirms that the two-step magnetic transition is not caused by the change of the relative strength between the magnetic contributions from the Np 5*f* electrons and other electrons in the ligand atoms, but occurs solely in the variation of the Np 5*f*-electron magnetic moment.

One can quantitatively estimate the values of μ_L and μ_S of the Np 5*f* electrons by applying the orbital and spin sum rules,[20,21,26]

$$\frac{\langle L_z\rangle}{3n_h} = \frac{\int_{M_4+M_5}\Delta\gamma(E)dE}{\frac{3}{2}\int_{M_4+M_5}\gamma(E)dE}, \quad (1)$$

$$\frac{2}{3}\frac{\langle S_z\rangle + 3\langle T_z\rangle}{n_h} = \frac{\int_{M_5}\Delta\gamma(E)dE - \frac{3}{2}\int_{M_4}\Delta\gamma(E)dE}{\frac{3}{2}\int_{M_4+M_5}\gamma(E)dE}, \quad (2)$$

to the integrated intensities of the $M_{4,5}$ XMCD and XAS spectra. Here, $\langle L_z\rangle$, $\langle S_z\rangle$, and $\langle T_z\rangle$ are the expectation values of the *z* component of the orbital angular momentum, the spin angular momentum, and the magnetic-dipole operator of the 5*f* shell, respectively. n_h is the number of holes in the 5*f* shell. $\gamma(E)$, which is equal to $[\gamma_+(E)+\gamma_-(E)]/2$, denotes the XAS spectrum. One problem in this analysis is that the hole number n_h and the magnetic-dipole term $\langle T_z\rangle$ cannot be experimentally determined. Especially in the analysis for the $d\rightarrow 5f$ transition, the magnitude of $\langle T_z\rangle$ is expected to be comparable to that of $\langle S_z\rangle$ and a different way of estimation of $\langle T_z\rangle$ results in a wide variation in the evaluated value of μ_S. Since the 5*f* electron occupation number n_f of the metallic Np compounds is expected to be between 3 and 4, we attempted to evaluate μ_L and μ_S in the case of the $5f^3$ (Np^{4+}) and $5f^4$ (Np^{3+}) configurations. It is assumed that the magnitude of $\langle T_z\rangle$ is proportional to $\langle S_z\rangle$ and the theoretically obtained values of the ratio $R_T=\langle T_z\rangle/\langle S_z\rangle$ are used, which are 0.6162 and 0.2779 for the free ions of the $5f^3$ and the $5f^4$ configurations, respectively, calculated with the intermediate coupling scheme.[38] Then, using Eqs. (1) and (2), $\mu_L=-\langle L_z\rangle\mu_B$, $\mu_S=-2\langle S_z\rangle\mu_B$, and the total magnetic moment $\mu_{TOT}=\mu_L+\mu_S$ can be estimated for the $5f^3$ and $5f^4$ configurations.

Table I summarizes the values of μ_L, μ_S, μ_{TOT}, and the ratio μ_L/μ_S estimated from the $M_{4,5}$ XAS and XMCD spectra of $NpNiGa_5$ at 22 K (the LM state) and 5 K (the HM state). Estimated values for both the $5f^3$ and $5f^4$ configurations indicate that μ_L and μ_S are antiparallel with each other and μ_{TOT} is parallel to μ_L. By comparing the estimated μ_{TOT} values to those from the previous magnetization[6] and neutron scattering[10] experiments in Table I, one can see that the values estimated for the $5f^4$ configuration are more consistent with the magnetization and neutron-scattering values than those estimated for the $5f^3$ configuration both in the LM and

HM states. Thus, the $M_{4,5}$ XMCD results suggest that the $5f^4$ configuration is more likely for $NpNiGa_5$ than the $5f^3$ configuration both in the LM and HM states. This is consistent with the estimation from the isomer shift in the ^{237}Np Mössbauer spectroscopy.[7]

If the $5f^4$ configuration is adopted, the ratio μ_L/μ_S is estimated to be −1.88 and −1.76 for the HM and LM states, respectively. Lander *et al.* proposed a universal tendency for the actinide series, where $|\mu_L/\mu_S|$ decreases with n_f from $5f^2$ to $5f^7$, taking values ~2.5 for the $5f^3$ configuration and ~1.8 for the $5f^4$ configuration, and examined it for the results of neutron-scattering experiments.[39] In the present $M_{4,5}$ XMCD result, the $|\mu_L/\mu_S|$ value agrees well with the universal value estimated for the $5f^4$ configuration. In the previous $N_{4,5}$ XMCD experiment on uranium monochalcogenides, we have estimated $\mu_L/\mu_S \approx -2.3$ for the $5f^3$ configuration.[35] Therefore, the XMCD experiments also support the universal decreasing tendency of $|\mu_L/\mu_S|$ with n_f and yield $|\mu_L/\mu_S|$ values which are in agreement with the above universal values. In addition, the increase of $|\mu_L/\mu_S|$ from the LM to HM states implies a slight decrease of n_f from the LM to HM states.

It is interesting to note that the μ_S value estimated from the magnetic Compton scattering becomes smaller in the HM state than in the LM state;[40,41] an opposite tendency to the present XMCD result. This implies a possible contribution of conduction-electron polarization to the spin magnetic moment[41] and also a possible difference in the values of $R_T=\langle T_z\rangle/\langle S_z\rangle$ between the LM and HM states.

B. Ga *K* XMCD

Figures 3(a) and 3(b) show the Ga *K* XAS and XMCD spectra, respectively, of $NpNiGa_5$ at 5 K (the HM state). In Fig. 3(b), the XMCD spectrum at 25 K (the LM state) is superimposed on the XMCD spectrum at 5 K after having normalized the spectra to the peak top. It should be noted that there are two different crystallographic sites for the Ga atoms and therefore the XMCD spectra observed here are averages over the contributions from both sites. The line shapes of the XAS spectra with parallel (γ_+) and antiparallel (γ_-) helicities are almost identical, indicating that the XMCD effect is very weak compared to that in the Np $M_{4,5}$ edges. Nevertheless, by taking the difference between γ_+ and γ_-, one can obtain a clear XMCD signal, in which the line shapes are composed of the major negative peak on the lower energy side and the slightly positive part on the higher energy side, as shown in Fig. 3(b). The observed line shapes are similar to those of the Ge *K* XMCD spectra of UGe_2 (Ref. 43) and the Ga *K* XMCD spectra of Mn_3GaC.[44,45] When the temperature is lowered from 25 K (the LM state) to 5 K (the HM state), the intensity of the XMCD signal increases by a factor of 1.56, while the line shapes remain almost unchanged.

The following orbital sum rule has been proposed for the XMCD at the *K* edge:[46,47]

$$\frac{3\langle L_z^p\rangle}{n_h^p} = \frac{\int_0^{\omega_c}\Delta\gamma(\omega)d\omega}{\int_0^{\omega_c}\gamma(\omega)d\omega}, \tag{3}$$

where $\langle L_z^p\rangle$ is the expectation value of the z component of the orbital angular momentum in the p-symmetry state and n_h^p is

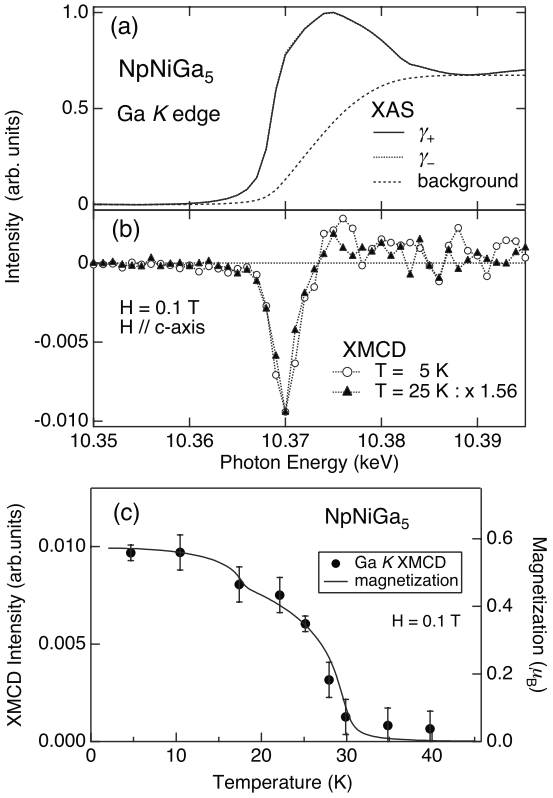

FIG. 3. XAS and XMCD spectra at the Ga *K* edge of $NpNiGa_5$ under a magnetic field applied along the *c* axis. (a) XAS spectra measured at 5 K with the photon helicity parallel (γ_+) and antiparallel (γ_-) to the applied magnetic field, respectively. (b) XMCD ($\Delta\gamma=\gamma_+-\gamma_-$) spectra at 5 and 25 K. (c) Temperature dependence of the intensity of the Ga *K* XMCD signal of $NpNiGa_5$ compared to the temperature dependence of the magnetization along the *c* axis (Ref. 6).

the hole number of the p states. ω_c is a cutoff frequency. Equation (3) means that the integrated intensity of the Ga *K* XMCD signal is proportional to the magnitude of the orbital magnetic moment μ_L of the Ga $4p$ electrons. Therefore, the present Ga *K* XMCD result indicates that the Ga $4p$ electrons have a finite orbital polarization. Similarly, the Ga $4p$ orbital polarization was claimed by the previous resonant x-ray scattering experiments on $NpCoGa_5$ and $NpRhGa_5$.[25] The negative value of the integrated Ga *K* XMCD intensity as shown in Fig. 3(b) indicates that the μ_L of the Ga $4p$ electrons is directed parallel to the applied magnetic field, accordingly parallel to the μ_L of the Np $5f$ electrons. If the numerator and denominator of the right-hand side of Eq. (3) are considered to be equal to the integrated intensities of the Ga *K* XAS and XMCD spectra, respectively, one can quantitatively estimate the value of μ_L. We adopt the integral-type background for the XAS spectrum to estimate the integrated intensity of the XAS spectrum, as shown in Fig. 3(a). This background-intensity estimation may cause an error in the XAS-intensity estimation because the background intensity is comparable to the XAS intensity. If the n_h^p value is assumed to be 5, the Ga $4p$ orbital moment is estimated to be $\mu_L=-\langle L_z^p\rangle\mu_B \approx 0.004\mu_B$. It should be noted that the quantitative applicability of the sum rule on the XMCD at *K* edge

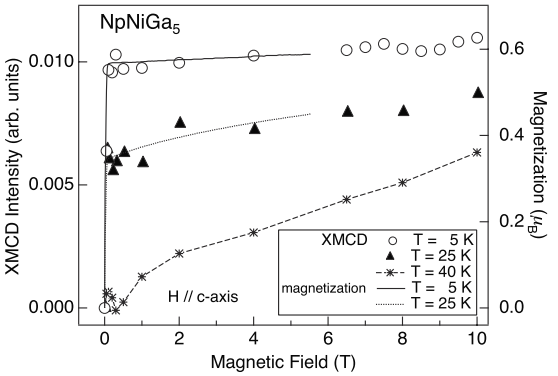

FIG. 4. Magnetic-field dependence of the intensity of the Ga K XMCD signal of $NpNiGa_5$ under a magnetic field applied along the c axis at 40 K (paramagnetic state), 25 K (LM state), and 5 K (HM state) compared to the magnetization along the c axis at 5 and 25 K (Ref. 6).

has not been established yet and should be a subject of further studies.

The temperature dependence of the Ga K XMCD intensity is plotted in Fig. 3(c). The Ga K XMCD signal also exhibits the two-step magnetic transition accompanied by intensity jumps at ~30 and ~12 K. The result indicates that the magnitude of the induced magnetic moment of the Ga $4p$ electrons varies nearly in proportion to the total magnetization of the system. Figure 4 displays the magnetic-field dependence of the Ga K XMCD intensity along the c axis at 40 K (paramagnetic state), 25 K (LM state), and 5 K (HM state). At 40 K, where the system is paramagnetic, it shows a linear increase. In the LM state (22 K) and the HM state (5 K), both of the plots show the ferromagnetic behavior; the intensity rapidly increases at the magnetic fields below 0.1 T and almost saturates above 0.1 T. The slope in the ordered region is larger in the LM state than in the HM state, consistent with the magnetization experiments.[6] Thus, Figs. 3(c) and 4 demonstrate that the Ga K XMCD signals serve as a precise probe of the total magnetization of the system.

IV. DISCUSSION

Table I demonstrates that the magnitude of $|\mu_L/\mu_S|$ deduced from the Np $M_{4,5}$ XMCD spectra is larger in the HM state than in the LM state. This difference might be related to the degree of delocalization of the Np $5f$ electrons. In the previous theoretical simulation by Yaouanc *et al.* applied to the $M_{4,5}$ XMCD study of the magnetic uranium compounds, it was shown that as the effective crystal-field parameter Δ becomes larger, $|\mu_L/\mu_S|$ for the $5f^2$ and $5f^3$ configurations becomes smaller.[48] In this simplified model, the uranium ions are supposed to be in an octahedral crystal field and the effective crystal-field parameter Δ was defined as the energy separation between the T_{2u} and A_{2u} levels, while the other parameters are kept to zero, resulting in a fixed energy for the T_{1u} level equals to $2\Delta/3$ above the T_{2u} level.[48] At the same time, a significant Δ dependence occurs in the line shapes of the M_5 XMCD signals for the $5f^2$ and $5f^3$ configurations: while the M_5 XMCD spectrum shows a dominant

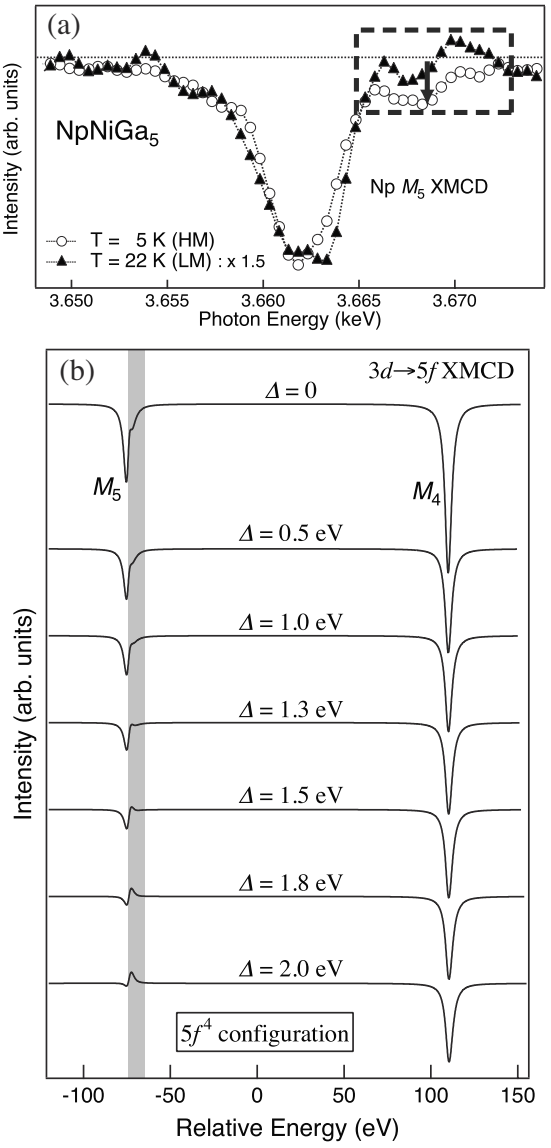

FIG. 5. (a) Magnified view of the line shapes of the Np M_5 XMCD spectra of $NpNiGa_5$ at 22 and 5 K. The high-energy part of the dominant negative peak is enclosed by broken lines. (b) Calculated $M_{4,5}$ XMCD spectra for the $5f^4$ configuration as a function of the effective crystal-field parameter Δ, obtained from the simulation same as in Ref. 48.

negative peak in the absence of Δ, the high-energy side of the dominant negative peak grows in the relatively positive intensity as Δ becomes larger.[48] The observation of *two lobes*, which are composed of the dominant negative peak and the positive peak at the high-energy side of the dominant negative peak, is an indication of a large Δ value.[48] Yaouanc *et al.* interpreted the physical meaning of Δ as the energy scale of the interaction of the $5f$ electrons with their environment, providing a measure for the crystal field and the strength of hybridization between the $5f$ and conduction-electron states (c-f hybridization).[48]

Figure 5(a) indicates a comparison between the LM (22 K) and HM (5 K) states in the line shapes of the Np M_5 XMCD spectra of $NpNiGa_5$. One can see that the high-energy side, enclosed by broken lines in Fig. 5, of the domi-

TABLE II. Tendencies between the LM and HM states observed in the magnetization along the c axis, the $|\mu_L/\mu_S|$ values estimated from the $M_{4,5}$ XMCD result, and the relative position of the high-energy part of the M_5 XMCD spectra, and a tendency expected for the effective crystal-field parameter Δ in the simulation same as in Ref. 48.

	LM	HM
Magnetization along c axis	small	large
$\|\mu_L/\mu_S\|$	small	large
High energy part of M_5 XMCD	more positive	more negative
Δ	large	small

nant negative peak is located at a slightly more negative intensity in the HM state (5 K) than in the LM state (22 K). In order to interpret this, we have calculated a Δ dependence of the $M_{4,5}$ XMCD spectra for the $5f^4$ configuration, as shown in Fig. 5(b), by the simulation in the same manner of Yaouanc *et al.*,[48] since Yaouanc *et al.* did not present the result for the $5f^4$ configuration. The gray zone in Fig. 5(b) demonstrates that the high-energy side of the dominant negative peak of the M_5 XMCD spectra is growing toward the positive intensity as the Δ becomes larger, same as in the case of the f^2 and f^3 configurations. Therefore, the observed tendency, that, in going from the LM to HM states, the intensity of the high-energy part in the Np M_5 XMCD spectrum become more negative and at the same time $|\mu_L/\mu_S|$ becomes larger, agrees with the result expected when Δ is decreased, as summarized in Table II. If it is supposed that the variation in the effective crystal-field parameter Δ is brought about by the variation in the c-f hybridization strength, the present result implies that the c-f hybridization strength is smaller in the HM state than in the LM state, presumably related to the enlargement of the magnetization along the c axis.

V. SUMMARY

We have measured XMCD at the Np $M_{4,5}$ and the Ga K edges of $NpNiGa_5$ in order to investigate the change of magnetic properties of the Np $5f$ and Ga $4p$ electrons depending on temperature. The temperature dependence of the Np M_4 XMCD intensity exhibits the two-step magnetic transition, confirming that the two-step magnetic transition occurs solely in the behavior of the Np $5f$ magnetic moments. From the analysis of the Np $M_{4,5}$ XMCD data, the following characteristics were clarified for the high-temperature LM state and the low-temperature HM state of $NpNiGa_5$:

(1) Comparing the magnetic moments in the sum-rule analysis of the XMCD data with the previous magnetization and the neutron-scattering results, it is concluded that the $5f^4$ (Np^{3+}) configuration is more likely than the $5f^3$ (Np^{4+}) configuration both for the LM and HM states.

(2) The ratio of the orbital to the spin magnetic moments is estimated to be $|\mu_L/\mu_S| \approx 1.7-1.9$ for the $5f^4$ configuration, which agrees well with the value in the general tendency of $|\mu_L/\mu_S|$ depending on the $5f$ electron counts.[39]

(3) $|\mu_L/\mu_S|$ tends to become larger in going from the LM state to the HM state.

(4) The decrease of the c-f hybridization strength from the LM to the HM states may be inferred, related to the observed increase of $|\mu_L/\mu_S|$ and the enlargement of the Np $5f$ magnetic moment along the c axis.

The magnetic polarization behavior of the p electrons in the ligand atom is observed by Ga K XMCD measurement. The Ga K XMCD intensity shows temperature and magnetic-field dependences nearly proportional to the total magnetization of the system.

ACKNOWLEDGMENTS

This work was performed under the Proposals No. 2006A1396 at BL39XU and No. 2007A3712 and No. 2007B3709 at BL22XU of SPring-8. The work at BL22XU was supported by the Grant-in-Aid for Scientific Research Contracts No. 19540383 and No. 20102003 from the Ministry of Education, Culture, Sports, Science, and Technology, Japan. This work was also supported by the HOUGA Research Resources of Japan Atomic Energy Agency.

*okanet@spring8.or.jp

†Present address: SPring-8/Japan Synchrotron Radiation Research Institute, Hyogo 679-5198, Japan.

‡Present address: INAC/SPSMS, CEA-Grenoble, 17 rue des Martyrs, 38054 Grenoble, France.

[1] J. L. Sarrao, L. A. Morales, J. D. Thompson, B. L. Scott, G. R. Stewart, F. Wastin, J. Rebizant, P. Boulet, E. Colineau, and G. H. Lander, Nature (London) **420**, 297 (2002).

[2] F. Wastin, P. Boulet, J. Rebizant, E. Colineau, and G. H. Lander, J. Phys.: Condens. Matter **15**, S2279 (2003).

[3] E. Colineau, P. Javorský, P. Boulet, F. Wastin, J. C. Griveau, J. Rebizant, J. P. Sanchez, and G. R. Stewart, Phys. Rev. B **69**, 184411 (2004).

[4] D. Aoki, Y. Homma, Y. Shiokawa, E. Yamamoto, A. Nakamura, Y. Haga, R. Settai, T. Takeuchi, and Y. Ōnuki, J. Phys. Soc. Jpn. **73**, 1665 (2004).

[5] D. Aoki, Y. Homma, Y. Shiokawa, E. Yamamoto, A. Nakamura, Y. Haga, R. Settai, and Y. Ōnuki, J. Phys. Soc. Jpn. **73**, 2608 (2004).

[6] D. Aoki, Y. Homma, Y. Shiokawa, H. Sakai, E. Yamamoto, A. Nakamura, Y. Haga, R. Settai, and Y. Ōnuki, J. Phys. Soc. Jpn. **74**, 2323 (2005).

[7] E. Colineau, J. P. Sanchez, F. Wastin, P. Boulet, and J. Rebizant, J. Phys.: Condens. Matter **19**, 246202 (2007).

[8] N. Metoki, K. Kaneko, E. Colineau, P. Javorský, D. Aoki, Y. Homma, P. Boulet, F. Wastin, Y. Shiokawa, N. Bernhoeft, E.

Yamamoto, Y. Ōnuki, J. Rebizant, and G. H. Lander, Phys. Rev. B **72**, 014460 (2005).
[9] S. Jonen, N. Metoki, F. Honda, K. Kaneko, E. Yamamoto, Y. Haga, D. Aoki, Y. Homma, Y. Shiokawa, and Y. Ōnuki, Phys. Rev. B **74**, 144412 (2006).
[10] F. Honda, N. Metoki, K. Kaneko, S. Jonen, E. Yamamoto, D. Aoki, Y. Homma, Y. Haga, Y. Shiokawa, and Y. Ōnuki, Phys. Rev. B **74**, 144413 (2006).
[11] Y. Tokiwa, Y. Haga, E. Yamamoto, D. Aoki, N. Watanabe, R. Settai, T. Inoue, K. Kindo, H. Harima, and Y. Ōnuki, J. Phys. Soc. Jpn. **70**, 1744 (2001).
[12] Y. Tokiwa, T. Maehira, S. Ikeda, Y. Haga, E. Yamamoto, A. Nakamura, Y. Ōnuki, M. Higuchi, and A. Hasegawa, J. Phys. Soc. Jpn. **70**, 2982 (2001).
[13] Y. Tokiwa, Y. Haga, N. Metoki, Y. Ishii, and Y. Ōnuki, J. Phys. Soc. Jpn. **71**, 725 (2002).
[14] R. Troć, Z. Bukowski, C. Sułkowski, H. Misiorek, J. A. Morkowski, A. Szajek, and G. Chełkowska, Phys. Rev. B **70**, 184443 (2004).
[15] N. O. Moreno, E. D. Bauer, J. L. Sarrao, M. F. Hundley, J. D. Thompson, and Z. Fisk, Phys. Rev. B **72**, 035119 (2005).
[16] K. Kaneko, N. Metoki, N. Bernhoeft, G. H. Lander, Y. Ishii, S. Ikeda, Y. Tokiwa, Y. Haga, and Y. Ōnuki, Phys. Rev. B **68**, 214419 (2003).
[17] P. Boulet, E. Colineau, F. Wastin, J. Rebizant, P. Javorský, G. H. Lander, and J. D. Thompson, Phys. Rev. B **72**, 104508 (2005).
[18] E. D. Bauer, J. D. Thompson, J. L. Sarrao, L. A. Morales, F. Wastin, J. Rebizant, J. C. Griveau, P. Javorský, P. Boulet, E. Colineau, G. H. Lander, and G. R. Stewart, Phys. Rev. Lett. **93**, 147005 (2004).
[19] P. Javorský, E. Colineau, F. Wastin, F. Jutier, J. C. Griveau, P. Boulet, R. Jardin, and J. Rebizant, Phys. Rev. B **75**, 184501 (2007).
[20] B. T. Thole, P. Carra, F. Sette, and G. van der Laan, Phys. Rev. Lett. **68**, 1943 (1992).
[21] P. Carra, B. T. Thole, M. Altarelli, and X. Wang, Phys. Rev. Lett. **70**, 694 (1993).
[22] M. van Veenendaal, Phys. Rev. B **67**, 134112 (2003).
[23] M. Usuda, J. I. Igarashi, and A. Kodama, Phys. Rev. B **69**, 224402 (2004).
[24] K. Kuzushita, K. Ishii, S. B. Wilkins, B. Janousova, T. Inami, K. Ohwada, M. Tsubota, Y. Murakami, K. Kaneko, N. Metoki, S. Ikeda, Y. Haga, Y. Ōnuki, N. Bernhoeft, and G. H. Lander, Phys. Rev. B **73**, 104431 (2006).
[25] B. Detlefs, S. B. Wilkins, R. Caciuffo, J. A. Paixão, K. Kaneko, F. Honda, N. Metoki, N. Bernhoeft, J. Rebizant, and G. H. Lander, Phys. Rev. B **77**, 024425 (2008).
[26] S. P. Collins, D. Laundy, C. C. Tang, and G. van der Laan, J. Phys.: Condens. Matter **7**, 9325 (1995).
[27] G. van der Laan, K. T. Moore, J. G. Tobin, B. W. Chung, M. A. Wall, and A. J. Schwartz, Phys. Rev. Lett. **93**, 097401 (2004).
[28] V. Antonov, B. Harmon, and A. Yaresko, *Electronic Structure and Magneto-Optical Properties of Solids* (Kluwer Academic Publishers, Dordrecht, 2004), Chap. 4.3.
[29] N. Kernavanois, P. Dalmas de Réotier, A. Yaouanc, J.-P. Sanchez, V. Honkimäki, T. Tschentscher, J. McCarthy, and O. Vogt, J. Phys.: Condens. Matter **13**, 9677 (2001).
[30] P. Dalmas de Réotier, J.-P. Sanchez, A. Yaouanc, M. Finazzi, Ph. Sainctavit, G. Krill, J. P. Kappler, J. Goedkoop, J. Goulon, C. Goulon-Ginet, A. Rogalev, and O. Vogt, J. Phys.: Condens. Matter **9**, 3291 (1997).
[31] M. Finazzi, Ph. Sainctavit, A.-M. Dias, J.-P. Kappler, G. Krill, J.-P. Sanchez, P. Dalmas de Réotier, A. Yaouanc, A. Rogalev, and J. Goulon, Phys. Rev. B **55**, 3010 (1997).
[32] M. Kučera, J. Kuneš, A. Kolomiets, M. Diviš, A. V. Andreev, V. Sechovský, J.-P. Kappler, and A. Rogalev, Phys. Rev. B **66**, 144405 (2002).
[33] A. N. Yaresko, P. Dalmas de Réotier, A. Yaouanc, N. Kernavanois, J.-P. Sanchez, A. A. Menovsky, and V. N. Antonov, J. Phys.: Condens. Matter **17**, 2443 (2005).
[34] T. Okane, J. Okamoto, K. Mamiya, S.-i. Fujimori, Y. Takeda, Y. Saitoh, Y. Muramatsu, A. Fujimori, Y. Haga, E. Yamamoto, A. Tanaka, T. Honma, Y. Inada, and Y. Ōnuki, J. Phys. Soc. Jpn. **75**, 024704 (2006).
[35] T. Okane, Y. Takeda, J. Okamoto, K. Mamiya, T. Ohkochi, S.-i. Fujimori, Y. Saitoh, H. Yamagami, A. Fujimori, A. Ochiai, and A. Tanaka, J. Phys. Soc. Jpn. **77**, 024706 (2008).
[36] P. Dalmas de Réotier, A. Yaouanc, G. van der Laan, N. Kernavanois, J.-P. Sanchez, J. L. Smith, A. Hiess, A. Huxley, and A. Rogalev, Phys. Rev. B **60**, 10606 (1999).
[37] A. Bombardi, N. Kernavanois, P. Dalmas de Réotier, G. H. Lander, J.-P. Sanchez, A. Yaouanc, P. Burlet, E. Lelièvre-Berna, A. Rogalev, O. Vogt, and K. Mattenberger, Eur. Phys. J. B **21**, 547 (2001).
[38] G. van der Laan and B. T. Thole, Phys. Rev. B **53**, 14458 (1996).
[39] G. H. Lander, M. S. S. Brooks, and B. Johansson, Phys. Rev. B **43**, 13672 (1991).
[40] S. Tsutsui, Y. Sakurai, M. Itou, D. Aoki, E. Yamamoto, Y. Homma, Y. Haga, A. Nakamura, Y. Shiokawa, and Y. Ōnuki, Physica B **378-380**, 1011 (2006).
[41] S. Tsutsui, Y. Sakurai, M. Itou, D. Aoki, E. Yamamoto, Y. Homma, Y. Haga, A. Nakamura, Y. Shiokawa, and Y. Ōnuki, J. Phys. Chem. Solids **68**, 2099 (2007).
[42] Errors in the estimated values were explicitly estimated only for the magnetic Compton scattering experiment as $\pm 0.08 \mu_B$. The errors in the μ_S values of the present XMCD study are presumably larger than those in the magnetic Compton scattering values, since the estimation of μ_S in the XMCD study uses the assumption on the $\langle T_z \rangle$ values.
[43] Y. Inada, T. Honma, N. Kawamura, M. Suzuki, H. Miyagawa, E. Yamamoto, Y. Haga, T. Okane, S. Fujimori, and Y. Ōnuki, Physica B **359-361**, 1054 (2005).
[44] N. Kawamura, N. Ishimatsu, M. Isshiki, Y. Komatsu, and H. Maruyama, Phys. Scr., T **115**, 591 (2005).
[45] M. Takahashi and J. I. Igarashi, Phys. Rev. B **67**, 245104 (2003).
[46] J. I. Igarashi and K. Hirai, Phys. Rev. B **50**, 17820 (1994).
[47] J. I. Igarashi and K. Hirai, Phys. Rev. B **53**, 6442 (1996).
[48] A. Yaouanc, P. Dalmas de Réotier, G. van der Laan, A. Hiess, J. Goulon, C. Neumann, P. Lejay, and N. Sato, Phys. Rev. B **58**, 8793 (1998).